J Mater Sci: Mater Med (2012) 23:1085–1096
DOI 10.1007/s10856-012-4559-9

Development of chitosan-tripolyphosphate non-woven fibrous scaffolds for tissue engineering application

Falguni Pati · Basudam Adhikari · Santanu Dhara

Received: 17 February 2011 / Accepted: 24 January 2012 / Published online: 7 February 2012

Abstract The fibrous scaffolds are promising for tissue engineering applications because of their close structural resemblance with native extracellular matrix. Additionally, the chemical composition of scaffold is also an important consideration as they have significant influences on modulating cell attachment, morphology and function. In this study, chitosan-tripolyphosphate (TPP) non-woven fibrous scaffolds were prepared through wetspinning process. Interestingly, at physiological pH these scaffolds release phosphate ions, which have significant influences on cellular function. For the first time, cell viability in presence of varying concentration of sodium TPP solution was analyzed and correlated with the phosphate release from the scaffolds during 30 days incubation period. In vitro degradation of the chitosan-TPP scaffolds was higher than chitosan scaffolds, which may be due to decrease in crystallinity as a result of instantaneous ionic cross-linking during fiber formation. The scaffolds with highly interconnected porous structure present a remarkable cytocompatibility for cell growing, and show a great potential for tissue engineering applications.

Keywords Chitosan-tripolyphosphate · Fibrous scaffold · Biodegradation · Cytotoxicity · Biocompatibility

F. Pati · S. Dhara (✉)
School of Medical Science and Technology, Indian Institute of Technology, Kharagpur 721302, India
e-mail: santanudhara@yahoo.co.in; sdhara@smst.iitkgp.ernet.in

B. Adhikari
Materials Science Centre, Indian Institute of Technology, Kharagpur 721302, India

1 Introduction

Three dimensional biopolymer scaffolds play an important role in tissue engineering (TE) for repairing, complementing and regenerating of diseased or traumatized tissue [1]. A significant attention is being given on tailoring the architecture, surface chemistry and tissue specific microenvironment of biopolymer scaffold, which facilitate cell-material interaction and eventually rebuilding of native tissues [2, 3]. Generally in TE, biopolymers are used in different forms like film, tape, gel, porous matrix/fibrous scaffolds of different architectures, porosity, permeability and topography [4]. The fiber-based architectures of scaffolds seem to be promising for tissue-engineering because of their close resemblance with native ECM [5]. Additionally, fibrous scaffolds are less prone to damage due to their inherent flexible nature and structural integrity. Further, highly interconnected open porous structures often facilitate optimized mass transport and cell migration into the core of the scaffolds [6]. Micro fibers have high surface to volume ratio, which account for enhanced cell-material interaction [7] and encourage maturation of cells with improved matrix production [8].

Various biopolymers have been encountered as scaffolding material in TE. Amongst them, chitosan has been extensively exploited for development of innovative biomatrices intended for clinical applications, such as drug delivery system (DDS) [9, 10], bioactive dressings [11, 12] and scaffolds for TE [13–17] owing to its high biocompatibility, biodegradability, antimicrobial activity, wound-healing potential and significant cellular activity [11, 13, 18]. Chitosan has been a very promising option for TE due to its structural similarities with glycosaminoglycans and hyaluronic acid present in human body [13–15]. Moreover, chitosan is susceptible to chemical or biological

functionalization due to the presence of amine functionality along the polymer backbone [19]. This biopolymer also shows a biological aptitude to stimulate cell proliferation and hystoarchitectural tissue organization and can play the role of biological primer for cell proliferation and tissue reconstruction [20]. Degradation of chitosan takes place by the action of several enzymes [21], but in vivo degradation is mainly attributed to the action of lysozyme [22]. However, the degradation of chitosan used to date in different applications is very slow and poorly controlled [23]. This is a significant limitation, as the degradation rate of polymeric matrices should match the rate of neo-tissue formation [24]. Chitosan's degradability can be tailored by manipulating the molecular weight and the degree of de-acetylation [21, 25]. However, it may lead to undesired changes in the properties of the polymer, such as cell-material interactions as it involves changes in the chemical structure of the material [26].

Chitosan fibers are generally spun in different alkaline media [27–30] and cross-linking of the fibers have also been proposed for improving the mechanical properties and tailoring biodegradation rate [31–33]. Being a polyanion, tripolyphosphate (TPP) is capable of interacting with polycationic chitosan by electrostatic forces [10]. However, sodium tripolyphosphate (STPP) has pH dependant ionization behavior owing to different pKa values (0.9, 1.9, 5.3, and 7.7) [34]. This pH dependant degree of ionization of TPP ions has strong influence on the mechanism of ionotropic gelation. Beyond pH 7.7, STPP is fully ionized and reacts kinetically with protonated chitosan and instantaneously formed chitosan-TPP gel. This principle of gel formation can be further extended to spinning of chitosan fibers and may be preferable over covalent cross-linking for prevention of possible toxicity and other undesirable effects [9]. There are very few literatures available on the preparation of chitosan fiber in STPP bath [35, 36], but, the cytotoxicity and biocompatibility were not studied in detail. Recently, ultrafine chitosan-TPP fibers were produced using a simple modified wetspinning technique and mechanism of fiber formation through ionotropic gelation was studied in detail under physiological condition by the authors as well [37, 38]. Interestingly, chitosan-TPP fibers are capable of releasing phosphate ions owing to the reversible complex formation of TPP ions with chitosan, which may have significant influence on modulating cell morphology, differentiation, and function. However the cytotoxicity, biocompatibility, cell attachment and proliferation on the chitosan-TPP fibrous scaffolds need to be elucidated for intended application in TE.

In the present study, chitosan-TPP fibers produced by wetspinning technique in STPP bath were used for preparation of non-woven fibrous scaffolds. The developed scaffolds were characterized by different physico-chemical techniques like FTIR, XRD and thermal analysis. In vitro degradation of the chitosan-TPP scaffolds were also evaluated in phosphate buffered saline (PBS) containing lysozyme. Cell viability in presence of varying concentration of sodium tripolyphosphate solution was analyzed and correlated with the phosphate release from the scaffold during 30 days incubation period for the first time. The biocompatibility is closely related to chemistry of materials and cell behavior on contact with them particularly cell adhesion to their surface [39]. The cell adhesion, proliferation, viability, morphology and mitochondrial function were analyzed after the culturing of 3T3 cells on chitosan-TPP fibrous scaffolds. Attachment of cells to the scaffolds was visualized by scanning electron microscopy (SEM) and fluorescence microscopy.

2 Materials and methods

2.1 Fabrication of chitosan-TPP fibrous scaffold

Chitosan stock solution (4 wt%) was prepared by dissolving required quantity of chitosan powder (Brookfield viscosity 800 cps, >75% deacytylated, high molecular weight, Sigma-Aldrich, Germany) in 2% acetic acid with constant overnight stirring. The homogeneous solution was filtered through a filter cloth, deaired by centrifugation and the solutions were kept at room temperature overnight for aging. Homogenous chitosan solution was spun into fiber using viscose type spinneret (50 holes, 0.1 mm hole diameter) in 5% (w/v) STPP (Loba Chemie, Mumbai, India) bath (pH 8.6). In addition, chitosan fibers were also spun in conventional alkaline bath, 5% (w/v) NaOH (pH 13) for comparative analysis. The fibers were collected and thoroughly washed with distilled water until the rinsed water exhibited a neutral pH. Fibers were incubated in gradation ethanol (50–100%) and used for scaffold fabrication.

Similar amount of fibers (by weight) were put into cylindrical polystyrene mould (16 mm i. d.) and excess ethanol was removed from the fibers. They were dried in an oven at 60°C overnight to obtain bulk chitosan fibrous scaffold. Chitosan-TPP and chitosan scaffolds obtained from STPP and NaOH bath were designated as C4S and C4N, respectively.

2.2 Scanning electron microscopy

The morphology and surface features of the scaffolds were examined using SEM (EVO 60, Carl ZEISS SMT, Germany). Prior to observation, samples were arranged on metal grids, using double-sided adhesive carbon tape, and coated with gold under vacuum.

2.3 Porosity determination

The porosity of C4S and C4N scaffolds was measured using a specific gravity bottle (Borosil Glass works Ltd., Mumbai, India) based on Archimedes' principle [40]. The porosity of the scaffold was determined as follows:

$$\text{Porosity}\,(\%) = [(W_2 - W_3 - W_s)/\rho_e]/[(W_1 - W_3)/\rho_e] \times 100$$

where W_1, the weight of the specific gravity bottle filled with ethanol; W_2, the weight of the specific gravity bottle including ethanol and the scaffold; W_3, the weight of specific gravity bottle when the ethanol saturated scaffold has been removed from W_2; W_s, weight of the scaffold; ρ_e, the density of ethanol, and thus; $(W_1-W_3)/\rho_e$, the total volume of the scaffold including pores; $(W_2-W_3-W_s)/\rho_e$, the pore volume in the scaffold.

2.4 FTIR analysis

The FTIR spectra of chitosan powder, C4S and C4N scaffold were recorded with KBr pellets on a FTIR spectrophotometer (Model-NEXUS-870, Thermo Nicolet Corporation, Madison, WI, USA). Each vacuum dried sample was mixed with ~5 times KBr powder and made into pellets by a hydraulic press.

2.5 Swelling studies

Swelling study of the scaffolds was carried out in incomplete Dulbecco's Modified Eagle's Media (DMEM, pH-7.4) at 37°C and 70–75% relative humidity until they reached saturated condition, a constant wet weight. At different time intervals (30 min, 1, 2, 4, 8, 12, 24 and 48 h), the scaffolds were weighed after wiping out the surface water with a tissue paper. The percentage swelling was calculated using the following formula:

$$\%\,\text{Swelling} = [(\text{wet weight} - \text{dry weight})/\text{dry weight}] \times 100.$$

2.6 XRD analysis

The X-ray diffraction patterns of chitosan powder, C4S and C4N scaffold were obtained using a X-ray diffractometer (Philips PANalytical X'Pert) using Nickel-filtered CuKα radiation at 40 kV and 50 mA in the 2θ range of 10–40°.

2.7 In vitro degradation study

The in vitro degradation of C4S and C4N scaffolds was carried out in phosphate-buffered solution (PBS, pH 7.4) at 37°C containing 1.5 μg/ml lysozyme (hen egg-white, Sigma-Aldrich, Steinheim, Switzerland) according to the procedure described elsewhere [26]. The concentration of lysozyme was chosen according to the concentration in human serum [41]. Briefly, scaffolds of known dry weights were sterilized by immersing in 70% alcohol followed by washing thoroughly with PBS (pH 7.4) and incubated in the lysozyme solution with gentle mechanical agitation for the period of study. The lysozyme solution was refreshed daily to ensure continuous enzyme activity [42]. At specified intervals (1, 4, 7, 15, 30 and 60 days) samples were removed from the medium, rinsed with distilled water, dried under vacuum and weighed. The extent of in vitro degradation was expressed as % residue of the dried scaffolds ($n = 3$ samples for each type) after lysozyme treatment. To distinguish between enzymatic degradation and dissolution, control samples were also stored for 60 days under the same conditions as described above, but without the addition of lysozyme.

2.8 Mechanical testing

Compressive strength of scaffolds in wet condition was measured on a universal testing machine (H25KS, Hounsfield, UK) at 25°C and 70–75% relative humidity. The scaffolds were rehydrated in PBS (pH 7.4) overnight prior to compression test. The height and diameter of the scaffolds were measured prior to the test. Scaffolds were compressed up to 70% of their initial height at a crosshead speed of 1 mm/min.

2.9 Thermo gravimetric analysis (TGA)

For estimation of inorganic residue, TGA of fully dried C4S scaffold before and after incubation for 15 and 30 days in incomplete media (DMEM) was performed with a Perkin Elmer Pyris Diamond TGA instrument, from 50 to 650°C, at a heating rate of 10°C/min. The open aluminum cell was swept with N_2 during the analysis.

2.10 Determination of phosphate release by spectrophotometric method

Total phosphate released from the C4S scaffolds was estimated through incubation of the scaffolds in double distilled water in 50 ml plastic tube for 30 days period with taking out samples at specified intervals (7, 15 and 30 days). Phosphate content in the samples was determined by the standard method described elsewhere [43]. Sample (2.5 ml) was transferred into the 50 ml volumetric flask followed by addition of 15 ml of a mixture of ammonium vanadate(V), ammonium molybdate(VI), nitric(V) acid and made up to the mark. Obtained solutions were left for 15 min to ensure color development and absorbance was measured at 430 nm against reagents blank.

The calibration curve was drawn using five working standards prepared from standard solution of STPP in the same way as above and calculated regression equation $y = 1.6359x + 0.4522$ was used for estimation of TPP release from samples. The calibration plots were linear in the concentration range from 0.1 to 5 mM STPP with the correlation coefficient of $R^2 = 0.992$.

2.11 Culture of 3T3 cells for biocompatibility assay

3T3 cells were adherent mouse fibroblasts that require a substratum for adherence and proliferation [44]. The cells were cultured in DMEM medium supplemented with 10% fetal bovine serum, 4 mM L-glutamine and 1% penicillin–streptomycin (A002A, Himedia, Mumbai, India) in tissue culture flasks at 37°C with 5% CO_2. The culture medium was changed every alternate day. Subculturing was done on every 3rd day by detaching cells from the flasks using trypsin–EDTA solution followed by splitting at 1:4 ratio. Before each experiment Trypan blue staining was used to check cell viability. Cells with >95% viability were used for further experiments.

2.11.1 Effect of STPP concentration on cell viability

The cell viability of 3T3 cells in presence of different concentration of TPP was evaluated by culturing the cells in six-well plate for 24 h and STPP solution of varying concentrations were added to each well. The concentration range of STPP was selected from 10 μM to 10 mM. Cell viability was measured through MTT assay [45] at specified intervals (6, 12 and 24 h) after addition of STPP. Briefly, the cells attached to the well were washed with sterile PBS and incubated in a mixture of 360 μl of PBS and 40 μl MTT solution (5 mg/ml) in PBS for 4 h at 37°C and 5% CO_2. The intense purple colored formazan derivatives formed were dissolved with 400 μl dimethyl sulfoxide for 15 min and the absorbance was measured at 590 nm with a micro plate reader (Recorders and Medicare Systems, India).

The viability and induction of apoptosis after 24 h was also observed by double stain apoptosis detection kit (Hoechst 33342/Propidium Iodide) under fluorescence microscopy [46]. Hoechst 33342, blue-fluorescence dye, stains the condensed chromatin in apoptotic cells more brightly than the chromatin in normal cells. Propidium iodide (PI), a red-fluorescence dye, is only permeant to dead cells. The staining pattern by using these dyes makes it possible to distinguish normal, apoptotic, and dead cell populations. In order to ensure a representative count, each well was divided into quarters, and two fields per quarter were photographed using a fluorescence microscope (Zeiss Axio Observer Z1, Carl Zeiss, Germany) at ×100 magnification.

2.11.2 Cell proliferation and morphology assay

The C4S and C4N scaffolds were placed at the bottom of a 12-well plate. The scaffolds were sterilized by soaking in 70% ethanol for 1 h, and finally rinsed in sterilized phosphate PBS solution for more than three times. For cell proliferation study, 3T3s were seeded on the 12-well culture plate fixed with the scaffolds and in tissue culture plate (TCP) without any scaffold as control with a cell density of 10^5 cells/well. The proliferation of 3T3s on the scaffolds and TCP was quantified after 1, 3, 5 and 7 days by MTT assay [45] following the procedure described above.

The cell number in the samples was assessed by quantifying DNA (7.7 pg DNA/cell) in the constructs using Hoechst 33342 dye (invitrogen) assay [47]. On the requisite days, samples were washed with sterile PBS. Each sample was then digested with 1 ml 1% w/v papain/0.09% disodium ethylenediaminetetraacetic acid (Na_2EDTA). Shortly after, 100 μl of the papain-digested solution was added into 2 ml Hoechst 33342 solution (1 μg/ml), the fluorescence intensity at 450 nm was measured by a fluorescent spectrophotometer (Cary Eclipse spectrofluorimeter, Varian, San Carlos, CA). The cell number in the samples was determined by referring to a calibration curve, which was prepared in advance by following the same method for known number of cells under similar incubation conditions.

The morphology of the adherent cells proliferating on the scaffolds was examined using SEM. To prepare the samples for SEM analysis, the samples were soaked in 2.5% glutaraldehyde in PBS solution for 4 h for cell fixing and dehydrated in an ascending series of ethanol aqueous solutions (50–100%) at room temperature. After vacuum-drying, the samples were observed under SEM (EVO 60, Carl ZEISS SMT, Germany).

2.11.3 Viability assay on fibrous scaffolds

Cell viability was assessed using a Live/Dead viability/cytotoxicity kit (Molecular Probes) using the manufacturer's protocol. Equal numbers of fibroblast cells (10^5) were seeded on each scaffold and TCP using a similar technique to that mentioned earlier. The cultures were incubated for 1, 3, 5 or 7 days in a humidified atmosphere containing 5% CO_2 at 37°C.

On the specified day, the cells were trypsinized and isolated from the scaffolds. The cell suspensions were centrifuged at 1,000 rpm and resuspended in 1 ml of fresh medium. 2 μl of 50 μM calcein-AM solution and 4 μl of 2 mM ethidium homodimer-1 were added per milliliter of cells and incubated for 30 min in the dark. The samples were analyzed by flow cytometry (FACS Calibur B–D using Cell Quest Pro software), measuring green

fluorescence emission for calcein (live cells) and red fluorescence emission for ethidium homodimer-1 (dead cells). Cells were gated (to exclude debris) and the voltage and compensation adjusted before final images were taken.

2.11.4 Fluorescence microscopy

Attachment of seeded cells on C4S and C4N fibrous scaffolds was verified using fluorescence microscopy after staining with rhodamine–phalloidin and Hoechst 33342 using manufacturer's protocol (Invitrogen, USA). The scaffolds were washed three times with PBS (pH 7.4), followed by incubation in 4% formaldehyde in PBS for 10 min. The samples were further washed with PBS and the cells attached to scaffolds were then permeabilized using 0.1% Triton X-100 for 5 min. The samples were preincubated with 1% BSA for 30 min followed by incubation with rhodamine–phalloidin for 20 min at room temperature. Scaffolds were washed with PBS and incubated in 5 μg/ml Hoechst 33342 solution for staining for 30 min. Fluorescence images of stained constructs were obtained using a fluorescence microscope (Zeiss Axio Observer Z1, Carl Zeiss, Germany) with ApoTome attachment at ×200 magnification.

2.12 Statistical analysis

All the quantitative results were obtained from triplicate samples. Data were expressed as a mean ± SD. For statistical analysis, a two-tailed Student's *t*-test was used. Differences were considered to be significant at $P < 0.05$.

3 Results and discussion

Chitosan is an aminated polysaccharide that is soluble in weak acids due to the protonation of the amino groups [12]. Poly- or multi-valent anions are therefore extensively used to develop ionically cross-linked chitosan scaffolds utilizing the cationic nature of protonated chitosan solutions. In this study, chitosan-TPP fibers spun in STPP coagulation bath through instantaneous gelation of the polymer governed by ionic cross-linking were used for fabrication of 3-D mesh scaffolds. The developed scaffolds were ~1 cm in diameter and ~2 mm thick (Fig. 1a). SEM microscopic observation of the scaffold revealed a nonaligned nest like structure with interconnected porosity (Fig. 1b). Porosity determination of the scaffolds revealed both C4S and C4N scaffolds were highly porous with ~89 and 92% porosity, respectively (Fig. 2a). The swelling of the C4S and C4N scaffolds in DMEM was 384.3 ± 23.2% and 526.6 ± 28.4%, respectively, at 48 h. The interconnected porous structure and high degree of porosity of the scaffolds can provide good nutrient and oxygen transfer throughout the porosity of the scaffolds, which results in better cell migration and production of ECM in the interior part of the scaffolds. Further in C4S scaffold, TPP ions were held by reversible complexation with the protonated chitosan, the release of phosphate ions was expected. The release of phosphate was evaluated for a period of 30 days and their effect on the cell viability was also assessed through an independent study. Influence of this associated phosphate within the scaffolds on the attachment and proliferation of cells was evaluated by culturing 3T3 cells. This system would have an advantage to apply for TE due to non-harmful condition throughout the development of scaffolds.

3.1 FTIR analysis

FTIR spectra of chitosan powder, C4S and C4N scaffolds are shown in Fig. 2b. FTIR analysis of chitosan powder and scaffolds revealed characteristic absorption bands at 1,664 and 1,573 cm^{-1} attributed to amide I (C = O) and amide II (N–H), respectively; 1,383 cm^{-1} credited to the distorting vibration of C–C bond. Absorption band at 2,923 cm^{-1} in chitosan powder, C4N and C4S scaffolds owing to asymmetrical stretching of $–CH_2–$. The wide absorption band around 3,435 cm^{-1} was due to the stretching vibration of O–H and N–H, present in chitosan powder, C4N and C4S scaffolds. But, the peak at 3,435 cm^{-1} becomes wider in C4N, indicating enhanced hydrogen bonding. The characteristic absorption bands of chitosan, a band associated with glycosidic linkage at

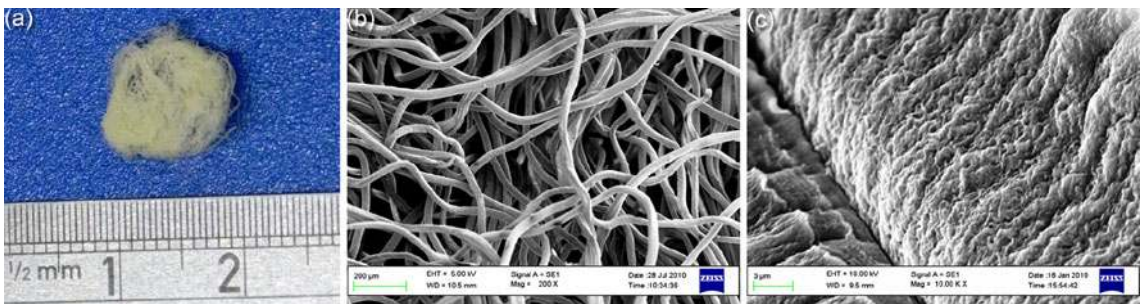

Fig. 1 **a** Digital image and SEM microscopic image of chitosan-TPP (C4S) scaffold at **b** ×200 and **c** ×10,000 magnification

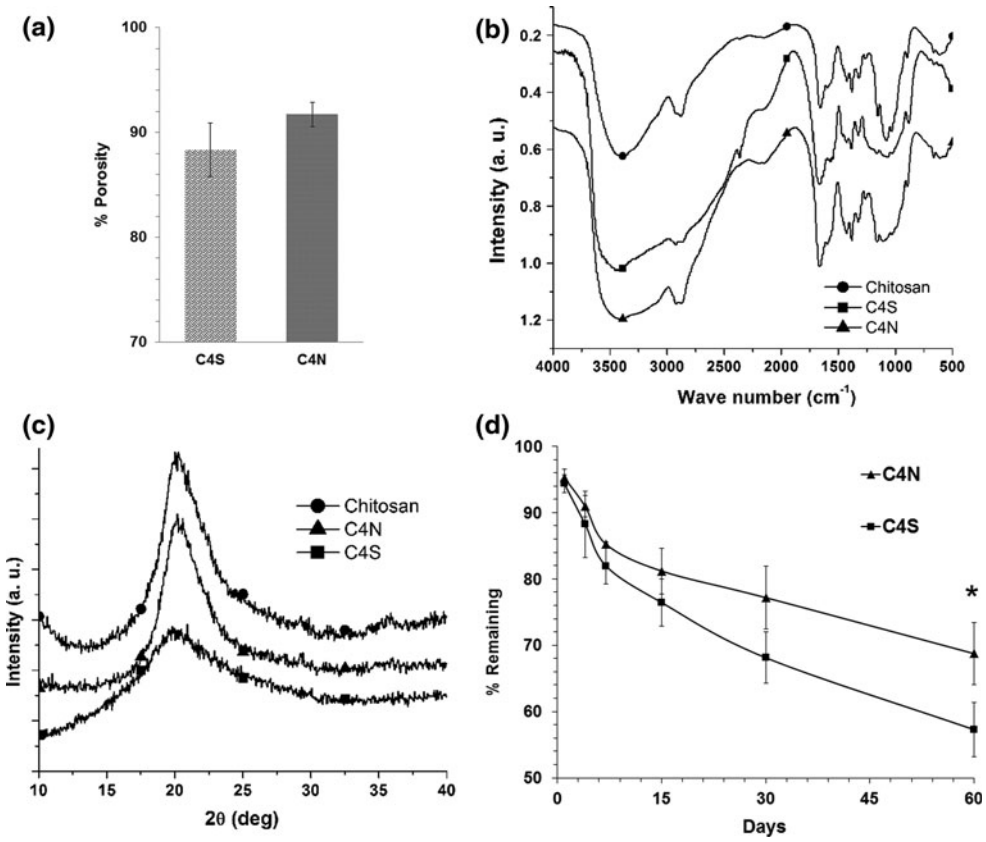

Fig. 2 **a** Percentage porosity of chitosan-TPP (C4S) and chitosan (C4N) scaffolds, **b** FTIR spectra of chitosan powder, C4S and C4N scaffolds, **c** XRD pattern of chitosan powder, C4S and C4N scaffolds and **d** in vitro degradation of C4S and C4N scaffolds

around 1,050 cm^{-1}, were present in chitosan powder and C4N scaffold. While in addition to that a sharp band appeared at 1,030 cm^{-1} in C4S scaffold, which is a characteristic P–O stretching band. The FTIR spectrum is consistent with the result of chitosan fiber modified by phosphate and is attributed to the linkage between phosphate and ammonium ion [48]. So, it is confirmed that the tripolyphosphates are linked with ammonium groups of chitosan in C4S fibers.

3.2 XRD analysis

The XRD patterns of chitosan powder, C4S fiber, C4N fiber are shown in Fig. 2c. The diffractogram of chitosan powder consisted of characteristic crystalline peak at 2θ value of 20.25°. XRD patterns revealed degree of crystallization of C4N fibers was relatively high in comparison to chitosan powder as peak intensity at 2θ value of 20.25° was increased, which may be due to orientation of the chitosan molecules along the direction of fiber drawing [49]. Interestingly, XRD pattern of C4S fibers (C4S) was more amorphous in nature as the peak intensity at 2θ value of 20.25° reduced. The difference in the diffraction patterns of C4S fibers from C4N fibers could be attributed to difference in molecular arrangement of polymer chains in presence of TPP molecules.

3.3 In vitro degradation study

The in vitro degradation behavior of C4S and C4N fibers was studied by incubating the fibers in lysozyme solution for a period of 60 days. As it can be seen in Fig. 2d, the % degradation of C4S was higher than that of C4N scaffold. In fact, at 60 day the differences in the weight loss profile of the three sets of scaffolds were not considered statistically significant ($P > 0.05$). This profile is probably due to the degradation phenomenon of the scaffolds themselves. The difference in degradation between C4S and C4N fibers may attributable to the degree of crystallinity of the fibers. As reported by Ren et al. [25], the degradation behavior of chitosan matrices depends on the crystallinity of chitosan because of the coexistence of the crystalline and amorphous zones in chitosan macromolecules. The degradation occurred first in amorphous zone followed by in the crystalline zone. So, the degradation rate of C4S and C4N fibers were different due to the difference in degree of crystallinity as evidenced in XRD analysis. The increase in rate of degradation of chitosan scaffolds without compromising the mechanical properties is advantageous from TE point of view.

3.4 Mechanical testing

Compressive strength of the scaffolds in wet condition was determined at a rate of 1 mm/min with a 100N load cell up to 70% of their initial height. The C4S scaffolds showed higher compressive strength (2.8 MPa) than that of C4N scaffolds (1.9 MPa) (Fig. 3a) because of the crosslinked nature of C4S scaffolds. A significant increase ($P < 0.05$) in compressive strength of C4S scaffolds was evidenced as a result of cross-linking by TPP ions.

3.5 Thermal analysis

Thermo-gravimetric analysis of dried C4S fibers before and after incubation in incomplete media (DMEM) was performed with a 10°C/min heating rate. A weight loss below and around 100°C for the samples was attributed to water evaporation (Fig. 3b). However, the weight loss above 200°C was due to the thermal decomposition of the materials. Thermo-gravimetric analysis was done for estimation of inorganic residue content before and after incubation in DMEM. C4S fibers contained significant amount of inorganic phosphate residue (~42%) even after heating up to 650°C as observed in Fig. 3b. When C4S fibers were incubated in DMEM, release of TPP ions was observed as the inorganic residue reduced to ~37 and ~35% after 15 and 30 days, respectively. So there is ~7% reduction in inorganic residue after 30 days incubation in DMEM due to the release of TPP ions from the fibers.

3.6 Total phosphate content

Total phosphate release from the C4S scaffolds was evaluated through incubation of the scaffolds in double distilled water for 30 days period and analyzed by spectrophotometric method. Phosphate release was found to be 0.4, 0.7 and 0.9 mM at 7, 15 and 30 days, respectively. So, total phosphate release was below 1 mM in 30 days study period, which was less than the toxic concentration of STPP found in MTT assay of cell cultured in presence of varying concentration of STPP.

3.7 Culture of 3T3 cells for biocompatibility assay

For TE application, the scaffold should not release any toxic products or produce adverse reactions, which could be evaluated through cytotoxicity tests. For evaluation of in vitro cytotoxicity, 3T3 cells were used as reference. The 3T3 cells were cultured for 7 days on the scaffolds for evaluation of cell attachment and proliferation and found encouraging results. The cell viability and proliferation were evaluated by MTT assay and DNA quantification using Hoechst 33342 dye, respectively, of the cell seeded scaffolds at specified intervals. As discussed previously, the TPP ions can be released from the C4S fibrous scaffolds, which can have influence on the growth rate and viability of cells. In this study, the growth rate and viability of the 3T3 cells were evaluated by culturing the cells in presence of different concentrations of STPP. At specified intervals, the viability was measured through MTT assay and visually observed through fluorescence microscopy.

3.7.1 Effect of STPP concentration on cell viability

3T3 cells were cultured on 6-well plate in presence of different concentration of STPP starting from 10 μM to 10 mM. From MTT assay, it was evidenced that the viability of cells cultured in presence of STPP concentration range up to 4 mM was similar to that of control, where no STPP has been added (Fig. 4a). Interestingly, at lower concentration (≤100 μM), STPP was found to enhance the

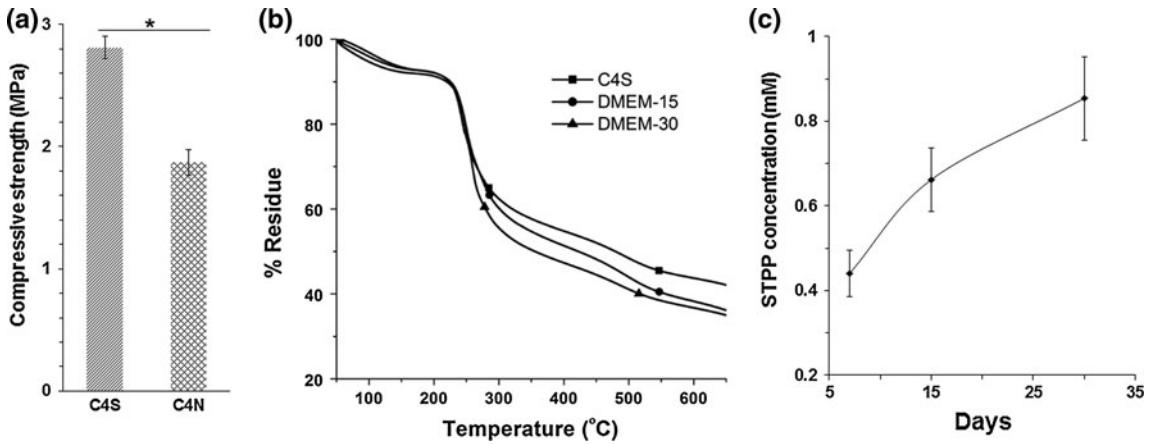

Fig. 3 **a** Compressive strength of chitosan-TPP (C4S) and chitosan (C4N) scaffolds (*$P < 0.05$), **b** thermo gravimetric analysis of C4S scaffold before and after incubation in incomplete media (DMEM) for 15 and 30 days, **c** phosphate release profile of C4S scaffold in double distilled water over a period of 30 days

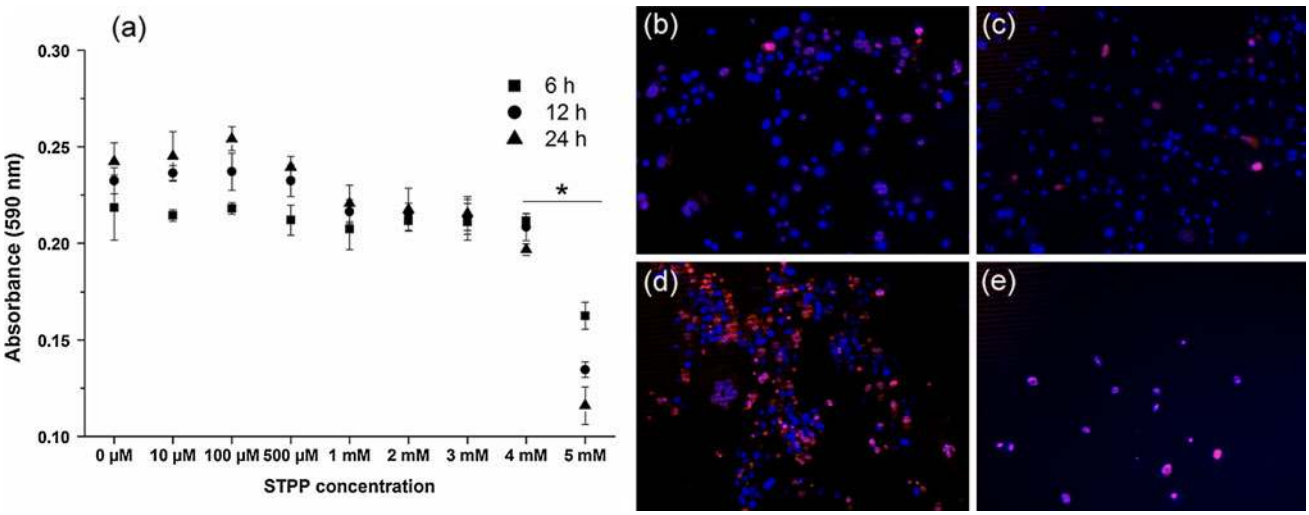

Fig. 4 **a** MTT assay of 3T3 cells cultured in presence of different concentration of STPP and fluorescence micrographs of treated cells after 24 h with STPP of **b** 100 µM, **c** 500 µM, **d** 5 mM and **e** 10 mM concentrations at ×100 magnification (*$P < 0.05$)

cell growth rate due to positive influence of lower phosphate concentration [50]. At 5 mM concentration of STPP, significant ($P < 0.05$) reduction in cell viability was observed than that of 4 mM due to toxic effect of TPP ions at this concentration. At further higher concentration (10 mM), maximum cells were dead when observed after 6 h under bright field inverted microscope (data not shown). From fluorescence micrographs, at STPP concentrations 100 and 500 µM there were very few cells were dead or apoptosis has been induced to a few cells (Fig 4b, c). But at 5 mM concentration ~50% cells were dead or apoptotic (Fig. 4d). At 10 mM concentration all cells were either dead or apoptotic (Fig. 4e). Thus, fluorescence microscopic results are in agreement with the MTT results obtained. So, 5 mM or higher concentration of STPP is toxic to the cells and could induce apoptosis.

3.7.2 Cell proliferation and morphology assay

The cell viability/proliferation of 3T3 cells cultured on the scaffolds and TCP, evaluated by MTT reduction assay and DNA quantifying assay using Hoechst 33342 dye are shown in Fig. 5. MTT is metabolized to a purple formazan salt by mitochondrial enzymes in living cells and the absorbance is proportional to the number of viable cells [45]. The absorbance value of MTT reduction assay of the cells seeded on C4S scaffolds was similar to the control cultures performed on TCP and was relatively higher than that of C4N scaffolds throughout the incubation period of 7 days (Fig. 5a). The absorbance value for the MTT reduction of the cultures grown on TCP decreased at the 7th day than that of C4S due to contact inhibition in the former case because of space constrains.

The proliferation rate of 3T3 cells grown on the C4S and C4N scaffolds and TCP are shown in Fig. 5b. Hoechst 33342 dye was used for evaluation of cell proliferation rate through analyzing the fluorescence intensity of the bound dye to DNA, which was proportional to number of cells in the scaffolds. The cells were able to attach and proliferate in both types of scaffolds. While comparing the cell proliferation rate amongst two types of scaffolds with TCP, C4S supported better cell proliferation similar to TCP and the cell proliferation was marginally less in C4N. As it can be seen, fibroblasts seeded on the C4S scaffolds showed relatively higher proliferation rate in MTT reduction assay and DNA quantifying assay than C4N scaffolds, which means metabolic activity and number of cells were higher in the former one. This may be an influence of the released phosphate ions from C4S scaffolds. This can also be related to the enhanced cell attachment on the C4S scaffolds. In fact, it has been reported that the proliferation rate of the cells was affected by initial cell attachment [51].

The cells attachment to the fiber surface was visualized under SEM microscope of glutaraldehyde fixed samples as shown in Fig. 5c. As observed by SEM, C4S fibers had supported better cell adhesion and growth, compared to C4N fibers, which was also evidenced in MTT reduction assay and DNA quantifying assay. The cells were observed to form a sheath on the scaffold in 8 days culture period, a sign of a high level of proliferation (Fig. 5c). It is assumed that the highly interconnected porous C4S and C4N scaffolds facilitated easy passage of nutrients to the proliferating cells and also aid in faster diffusion out of waste products from the inner core. In this study, cell adherence and proliferation in C4S scaffolds were better and were observed to be growing normally in comparison to the control.

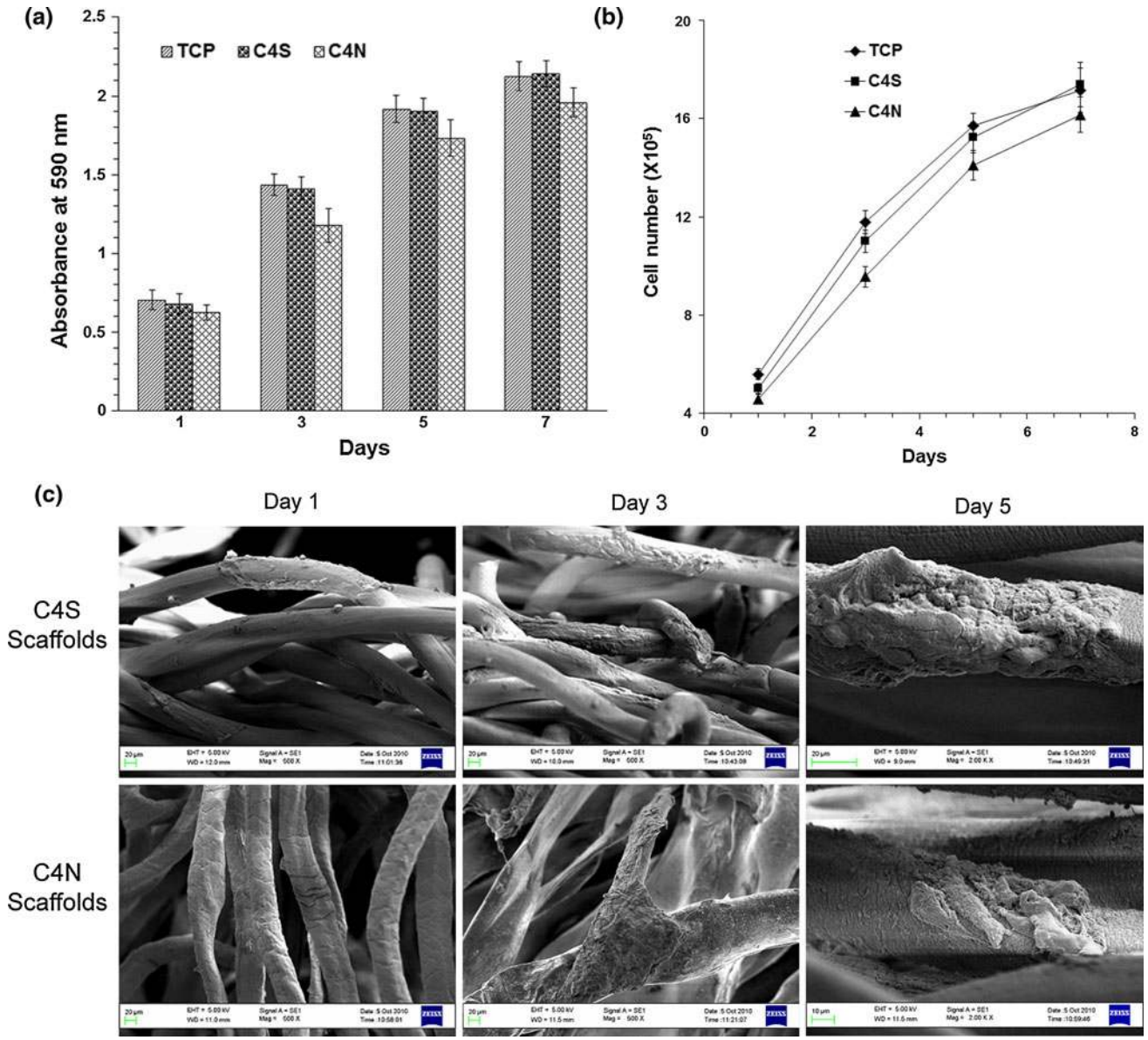

Fig. 5 **a** MTT reduction assay and **b** cell proliferation rate of 3T3 cells cultured on tissue culture plate (TCP), chitosan-TPP (C4S) and chitosan (C4N) fibrous scaffolds and **c** attachment of 3T3 cells on the fiber surface of C4S and C4N scaffolds

3.7.3 Viability assay on fibrous scaffolds

The biocompatibility of scaffolds was assessed through determination of cellular responses for application in TE. Live/Dead assay was carried out for evaluation of cellular response on the scaffolds using Live/Dead Kit from Molecular Probes and analyzed through flow cytometry (Fig. 6). On day 1, nearly 96% of the cells were alive on the control, and similar results were observed in C4S and C4N scaffolds, with 95 and 94% viable cells, respectively. On day 3, cell viability was slightly reduced in all cases and similar results were observed, with cell viabilities of 89, 87 and 86% for control, C4S and C4N, respectively. Cell viability was further decreased on days 5 and 7 for the control as well as in case of C4S and C4N scaffolds. This is due to the limited surface area for attachment of proliferating cells on control plates. As already observed in MTT and DNA quantification assay, cells on the control and scaffolds attained a higher density on day 5 and 7 due to the faster growth rate. Thus, due to the lack of sufficient surface for adherence of greater number of cells, viability was less at the end of days 5 and 7 on control culture. In comparison, the fibrous scaffolds continued to support cells and at the end of day 7 the percentage of viable cells was higher than that on the controls, with nearly 75 and 73% live cells in C4S and C4N scaffolds, respectively, compared to 70% in case of control plates. Interestingly, C4S scaffolds supported better cell

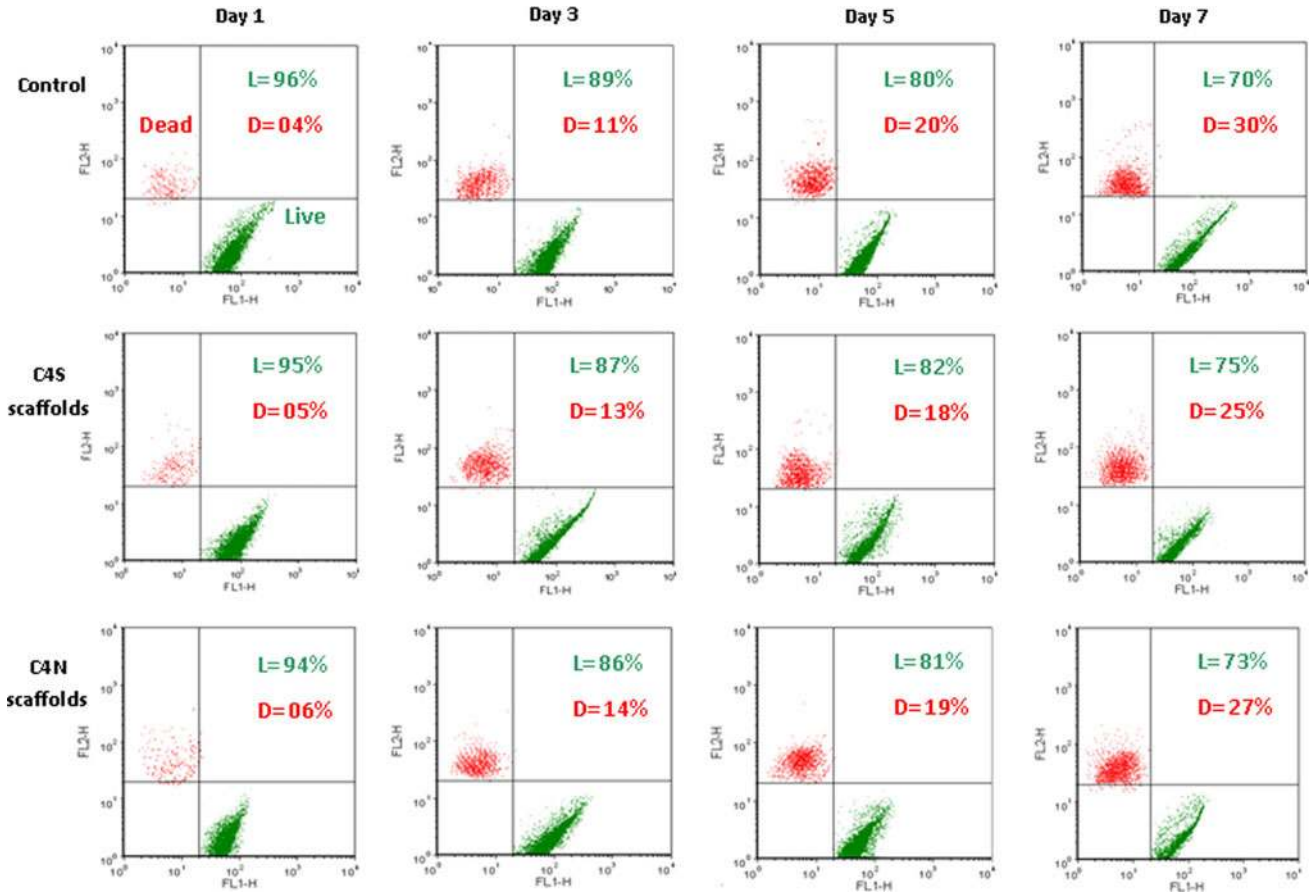

Fig. 6 Flow cytometric viability assay of 3T3 cells on chitosan-TPP (C4S) and chitosan (C4N) scaffolds and polystyrene plate as a control. The green dots represent viable cells (calcein-AM stained) and red dots represent dead cells (ethidium homodimer 1 stained). The percentage of viable and dead cells are shown in the inset in each representative figure (*L* live; *D* dead)

attachment and proliferation throughout the period of study in comparison to C4N scaffolds. The results further support the earlier findings of the MTT assays and DNT quantification, which showed that C4S scaffolds supported better cell attachment and viability. The results were comparable, and better than the controls on day 7. However, the decreasing viability with the time progression may due to the inhibition of trypsinization effect to all areas of scaffolds. Since cell lines proliferate well and produce a high amount of extracellular matrix with time, trypsinization will not reach the whole amount of cells, which may influences the results. This result further emphasizes that these scaffolds are suitable for cell culture applications as they allow nutrients and growing cells to pass through and reach the innermost core for growth and proliferation.

3.8 Fluorescence microscopy

Cells were firmly attached to the high surface area provided by fibrous scaffolds, i.e. C4S and C4N, as observed by fluorescence microscopy (Fig. 7). The fluorescence microscopic image of attached cells on the scaffolds is complementary with the earlier SEM results. Cells were observed to attach firmly on fibrous scaffolds with elongated morphology suggesting normal attachment, proliferation and growth. At 5th day, the scaffolds were fully covered with the cells, as observed in Fig. 7. Distinct rounded nuclei (blue colored) were observed throughout the scaffolds with well spread out actin filaments (red colored) suggesting cell proliferation and migration on the fiber surface. From SEM and fluorescence microscopy, attachment and spreading of fibroblast cells on C4S fibrous scaffolds was evidenced, which is a prerequisite for their application in TE.

4 Conclusions

The chitosan-TPP non-woven fibrous scaffolds were successfully prepared through wetspinning process. The scaffolds were highly porous ($\sim$89%) with interconnected open porous structure and had compressive strength of $\sim$2.9 MPa in hydrated condition. In vitro degradation of the chitosan-TPP scaffolds was improved in comparison to

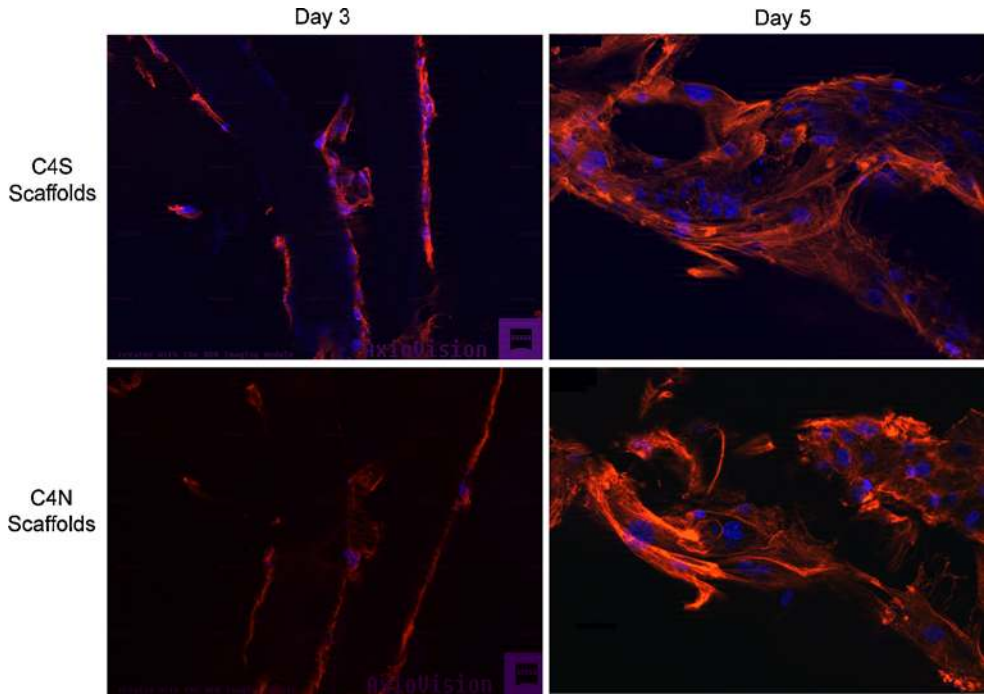

Fig. 7 Attached 3T3 cells on the chitosan-TPP (C4S) and chitosan (C4N) scaffolds after 3 days and 5 days of culture (×200 Magnification)

chitosan scaffold mainly due to decrease in crystallinity as a result of instantaneous ionic cross-linking during fiber formation. Further, the effect of STPP concentration on cell viability was also evaluated and ≥5 mM concentration was found to be toxic for 3T3 cells as evidenced by MTT and double stain apoptosis assay. Interestingly, chitosan-TPP scaffolds supported better cell attachment and growth than the chitosan scaffolds, which may be an outcome of incorporated phosphate ions. From SEM and fluorescence microscopy, cells were observed to attach firmly on the scaffolds with an elongated morphology. Altogether, these results suggested that C4S scaffolds are significantly biocompatible in nature and are suitable for TE application.

Acknowledgments Authors would like to acknowledge DBT and DST, Government of India for financial support and IIT Kharagpur for providing infrastructural facility. Finally, all lab members of Tissue Engineering laboratory at SMST, IIT Kharagpur are acknowledged for support.

References

1. Vacanti JP, Langer R. Tissue engineering: the design and fabrication of living replacement devices for surgical reconstruction and transplantation. Lancet. 1999;354:S32–4.
2. Kim B-S, Mooney DJ. Development of biocompatible synthetic extracellular matrices for tissue engineering. Trends Biotechnol. 1998;16(5):224–30.
3. Liu C, Xia Z, Czernuszka JT. Design and development of three-dimensional scaffolds for tissue engineering. Chem Eng Res Des. 2007;85(7):1051–64.
4. Tabata Y. Biomaterial technology for tissue engineering applications. J R Soc interface. 2009;6:S311–24.
5. Tuzlakoglu K, Reis RL. Biodegradable polymeric fiber structures in tissue engineering. Tissue Engineering Part B Rev. 2009;15(1):17–27.
6. Mikos AG, Sarakinos G, Lyman MD, Ingber DE, Vacanti JP, Langer R. Prevascularization of porous biodegradable polymers. Biotechnol Bioeng. 1993;42(6):716–23. doi:10.1002/bit.260420606.
7. Desai K, Kit K, Li J, Zivanovic S. Morphological and surface properties of electrospun chitosan nanofibers. Biomacromolecules. 2008;9(3):1000–6. doi:10.1021/bm701017z.
8. Ragetly GR, Griffon DJ, Lee H-B, Fredericks LP, Gordon-Evans W, Chung YS. Effect of chitosan scaffold microstructure on mesenchymal stem cell chondrogenesis. Acta Biomater. 2010;6(4):1430–6.
9. Berger J, Reist M, Mayer JM, Felt O, Peppas NA, Gurny R. Structure and interactions in covalently and ionically crosslinked chitosan hydrogels for biomedical applications. Eur J Pharm Biopharm. 2004;57(1):19–34.
10. Kawashima Y, Handa T, Kasai A, Takenaka H, Lin SY, Ando Y. Novel method for the preparation of controlled-release theophylline granules coated with a polyelectrolyte complex of sodium polyphosphate-chitosan. J Pharm Sci. 1985;74(3):264–8.
11. Muzzarelli RAA. Chitins and chitosans for the repair of wounded skin, nerve, cartilage and bone. Carbohydr Polym. 2009;76(2):167–82.
12. Ong S-Y, Wu J, Moochhala SM, Tan M-H, Lu J. Development of a chitosan-based wound dressing with improved hemostatic and antimicrobial properties. Biomaterials. 2008;29(32):4323–32.
13. Francis Suh JK, Matthew HWT. Application of chitosan-based polysaccharide biomaterials in cartilage tissue engineering: a review. Biomaterials. 2000;21(24):2589–98.
14. Lahiji A, Sohrabi A, Hungerford DS, Frondoza CG. Chitosan supports the expression of extracellular matrix proteins in human

osteoblasts and chondrocytes. J Biomed Mater Res. 2000; 51(4):586–95.
15. Malafaya P, Pedro A, Peterbauer A, Gabriel C, Redl H, Reis R. Chitosan particles agglomerated scaffolds for cartilage and osteochondral tissue engineering approaches with adipose tissue derived stem cells. J Mater Sci Mater Med. 2005;16(12):1077–85. doi:10.1007/s10856-005-4709-4.
16. Tuzlakoglu K, Alves CM, Mano JF, Reis RL. Production and characterization of chitosan fibers and 3-D fiber mesh scaffolds for tissue engineering applications. Macromol Biosci. 2004;4(8):811–9. doi:10.1002/mabi.200300100.
17. Di Martino A, Sittinger M, Risbud MV. Chitosan: a versatile biopolymer for orthopaedic tissue-engineering. Biomaterials. 2005;26(30):5983–90.
18. Hirano S, Seino H, Akiyama Y. Chitin and chitosan: ecologically bioactive polymers. Biotechnology and Bioactive Polymers. New York: Plenum Press; 1994.
19. Anwer K, Rhee BG, Mendiratta SK. Recent progress in polymeric gene delivery systems. Crit Rev Ther Drug Carrier Syst. 2003;20(4):249–93.
20. Muzzarelli R, Baldassarre V, Conti F, Ferrara P, Biagini G, Gazzanelli G, et al. Biological activity of chitosan: ultrastructural study. Biomaterials. 1988;9(3):247–52.
21. Zhang H, Neau SH. In vitro degradation of chitosan by a commercial enzyme preparation: effect of molecular weight and degree of deacetylation. Biomaterials. 2001;22(12):1653–8.
22. Vårum KM, Myhr MM, Hjerde RJN, Smidsrød O. In vitro degradation rates of partially N-acetylated chitosans in human serum. Carbohydr Res. 1997;299(1–2):99–101.
23. Tomihata K, Ikada Y. In vitro and in vivo degradation of films of chitin and its deacetylated derivatives. Biomaterials. 1997;18(7): 567–75.
24. Mi F-L, Tan Y-C, Liang H-F, Sung H-W. In vivo biocompatibility and degradability of a novel injectable-chitosan-based implant. Biomaterials. 2002;23(1):181–91.
25. Ren D, Yi H, Wang W, Ma X. The enzymatic degradation and swelling properties of chitosan matrices with different degrees of N-acetylation. Carbohydr Res. 2005;340(15):2403–10.
26. Freier T, Koh HS, Kazazian K, Shoichet MS. Controlling cell adhesion and degradation of chitosan films by N-acetylation. Biomaterials. 2005;26(29):5872–8.
27. Agboh OC, Qin Y. Chitin and chitosan fibers. Polym Advan Technol. 1997;8(6):355–65. doi:10.1002/(sici)1099-1581(199706)8:6<355:aid-pat651>3.0.co;2-t.
28. El-Tahlawy K, Hudson SM. Chitosan: aspects of fiber spinnability. J Appl Polym Sci. 2006;100(2):1162–8. doi:10.1002/app.23201.
29. Goosen MFA. Applications of chitin and chitosan. Lancaster: Technomic Publishing; 1997.
30. Hirano S, Nagamura K, Zhang M, Kim SK, Chung BG, Yoshikawa M, et al. Chitosan staple fibers and their chemical modification with some aldehydes. Carbohydr Polym. 1999;38(4): 293–8.
31. Knaul JZ, Hudson SM, Creber KAM. Improved mechanical properties of chitosan fibers. J Appl Polym Sci. 1999;72(13):1721–32.
32. Wei YC, Hudson SM, Mayer JM, Kaplan DL. The crosslinking of chitosan fibers. J Polym Sci A Polym Chem. 1992;30(10): 2187–93. doi:10.1002/pola.1992.080301013.
33. Yang Q, Dou F, Liang B, Shen Q. Studies of cross-linking reaction on chitosan fiber with glyoxal. Carbohydr Polym. 2005;59(2):205–10.
34. Martell AE, Smith RM. NIST Critically Selected Stability Constants of Metal Complexes Database. Gaithersburg: U.S. Dept. of Commerce; 2004.
35. Wang Q, Zhang N, Hu X, Yang J, Du Y. Chitosan/starch fibers and their properties for drug controlled release. Eur J Pharm Biopharm. 2007;66(3):398–404.
36. Yeh C-H, Lin P-W, Lin Y-C. Chitosan microfiber fabrication using a microfluidic chip and its application to cell cultures. Microfluid Nanofluid. 2010;8(1):115–21. doi:10.1007/s10404-009-0485-7.
37. Pati F, Adhikari B, Dhara S. Development of ultrafine chitosan fibers through modified wetspinning technique. J Appl Polym Sci. 2011;121(3):1550–7.
38. Pati F, Adhikari B, Dhara S. Development of chitosan–tripolyphosphate fibers through pH dependent ionotropic gelation. Carbohydr Res. 2011;346(16):2582–8. doi:10.1016/j.carres.2011.08.028.
39. Hubbell JA. Synthetic biodegradable polymers for tissue engineering and drug delivery. Curr Opinion Solid State Mater Sci. 1998;3(3):246–51.
40. Yang J, Shi G, Bei J, Wang S, Cao Y, Shang Q, et al. Fabrication and surface modification of macroporous poly(L-lactic acid) and poly(L-lactic-co-glycolic acid) (70/30) cell scaffolds for human skin fibroblast cell culture. J Biomed Mater Res. 2002;62(3): 438–46.
41. Brouwer J, van Leeuwen-Herberts T, Ruit MO-v. Determination of lysozyme in serum, urine, cerebrospinal fluid and feces by enzyme immunoassay. Clin Chim Acta. 1984;142(1):21–30.
42. Masuda T, Ueno Y, Kitabatake N. Sweetness and enzymatic activity of lysozyme. J Agric Food Chem. 2001;49(10):4937–41. doi:10.1021/jf010404q.
43. Marczenko Z, Balcerzak M. Separation, preconcentration, and spectrophotometry in inorganic analysis. Amsterdam: Elsevier; 2000.
44. Riley PA. The effect on cell proliferation of reduced substrate adhesiveness. Cell Differ. 1974;3(4):233–8.
45. Ciapetti G, Cenni E, Pratelli L, Pizzoferrato A. In vitro evaluation of cell/biomaterial interaction by MTT assay. Biomaterials. 1993;14(5):359–64.
46. Anestål K, Arnér ES. Rapid induction of cell death by selenium-compromised thioredoxin reductase 1 but not by the fully active enzyme containing selenocysteine. J Biol Chem. 2003;278(18): 15966–72.
47. Kim Y-J, Sah RLY, Doong J-YH, Grodzinsky AJ. Fluorometric assay of DNA in cartilage explants using Hoechst 33258. Anal Biochem. 1988;174(1):168–76.
48. Schauer CL, Chen M-S, Chatterley M, Eisemann K, Welsh ER, Price RR, et al. Color changes in chitosan and poly(allyl amine) films upon metal binding. Thin Solid Films. 2003;434(1–2):250–7.
49. Zhang X, Hua H, Shen X, Yang Q. In vitro degradation and biocompatibility of poly(l-lactic acid)/chitosan fiber composites. Polymer. 2007;48(4):1005–11.
50. Cheung HS, Tofe AJ. Mechanism of cell growth on calcium phosphate particles: role of cell-mediated dissolution of calcium phosphate matrix. STP Pharm Sci. 1993;3(1):51–5.
51. Anselme K. Osteoblast adhesion on biomaterials. Biomaterials. 2000;21(7):667–81.